

# Dipolar interactions in model Langmuir–Blodgett films

R. W. Munn and M. M. Shabat<sup>a)</sup>

Department of Chemistry and Center for Electronic Materials, UMIST, Manchester M60 1QD, United Kingdom

(Received 10 June 1993; accepted 30 August 1993)

Planewise dipole sums give the electric field at a point due to an array of electric dipole moments in a plane. Calculations are reported for model lattice structures of Langmuir–Blodgett films with elongated molecules represented by a string of spherical “beads” or submolecules; interactions are averaged over submolecules. Results are given for parent hexagonal and tetragonal lattices, with molecules allowed to tilt away from the vertical and with the in-layer cell parameters allowed to distort from equality. Beyond about five submolecules, molecular length makes little difference. Interactions within a layer dominate, with those between adjacent layers much smaller and those between remoter layers negligible. Tilt affects the interactions more than the detailed lattice structure does. The results provide a key ingredient for theories of the optical and electrical properties of Langmuir–Blodgett films.

## I. INTRODUCTION

Langmuir–Blodgett (LB) films offer an attractive method of designing molecular materials for various applications. Elongated amphiphilic molecules adsorb at the surface of a liquid subphase. The floating monolayer can be compressed and transferred to a solid substrate. Repetition of this process gives a multilayer assembly, which may be constructed from alternating different layers to afford a noncentrosymmetric material. Such materials exhibit properties such as pyroelectricity and optical second-harmonic generation, which one may seek to enhance by incorporating suitable functional groups.

Molecular materials have properties that arise from the molecular properties, the molecular arrangement, and the molecular interactions.<sup>1</sup> Designing molecular materials therefore requires an understanding of all these factors. For many optical and electrical properties of molecular crystals, the interaction of permanent or induced dipole moments plays an important role.<sup>2</sup> One then requires calculations of the electric field produced at a molecule due to dipole moments on the other molecules, which is determined by a *dipole sum*.

Similar considerations apply to Langmuir–Blodgett films. However, for these materials it is natural to adopt a planewise approach.<sup>3</sup> One then calculates the planewise dipole sum that gives the electric field produced at a molecule in one layer due to dipole moments on the molecules in that or another layer. Such an approach is related in a natural way to the method of deposition and to the structure of the films, and allows different numbers of layers to be treated. A planewise approach is also expected to be tractable rather than just conceptually attractive, since planewise dipole sums for aromatic hydrocarbon crystals fall off very rapidly with the separation between planes<sup>4</sup>—so rapidly that they offer an efficient means of calculating bulk lattice dipole sums.

We have previously indicated how to use planewise dipole sums to calculate optical properties.<sup>3</sup> In the present paper we report numerical calculations of planewise dipole sums for simple model Langmuir–Blodgett films. The results show how large the components of the sums are, how rapidly they fall off with the separation between layers, how they depend on the length of the molecules, and how they vary as the molecules tilt away from the normal to the layer. Selected results are used in the accompanying paper<sup>5</sup> to calculate the optical behavior of the model films. Preliminary reports of this work have appeared elsewhere;<sup>6,7</sup> it forms part of a program to design, prepare, and characterize Langmuir–Blodgett films for nonlinear optics.

## II. MODEL STRUCTURE

Langmuir–Blodgett films are known to be compact and well ordered. This suggests that for present purposes it should suffice to model the film structure as a layered crystal. It is then desirable that the crystal structure should reflect the molecular packing, taking account in particular of the elongation typical of molecules that afford LB films. The effect of molecular elongation has been examined previously in studies of linear optics of liquid crystals<sup>8</sup> and of nonlinear optics of molecular crystals.<sup>9</sup> The model adopted here is a variant of that considered in the previous papers.

Each molecule is treated as a string of  $s$  spherical submolecules or “beads” of diameter  $D$ . The submolecules serve as interaction centers; varying  $s$  changes the axial ratio of the molecule. In the parent structure of a layer, the molecules form a close-packed triangular array with their long axes perpendicular to the layer. In this arrangement the molecules are referred to as vertical. In the next layer the molecules are centered over the molecules in the first layer, and so on. The overall structure then has hexagonal symmetry. In the previous work,<sup>8</sup> the hemispherical base of a molecule in one layer touched the hemispherical caps of the molecules forming the triangle in the layer below. Here this refinement is ignored for simplicity, and instead the bases of one layer touch the tangent plane to the caps

<sup>a)</sup>Present address: The Islamic University of Gaza, P.O. Box 108, Gaza, Gaza Strip, via Israel.

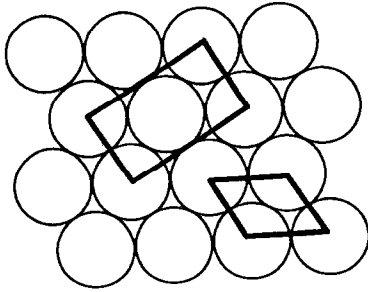


FIG. 1. Hexagonal parent model structure shown in plan with hexagonal and monoclinic unit cells.

in the layer below. As a result, the structure does not reduce to exact hexagonal close packing for  $s=1$ .

The model structure is illustrated in Fig. 1. It corresponds to a crystal with conventional lattice parameters  $a=b=D$ ,  $c=sD$ ,  $\alpha=\beta=90^\circ$ , and  $\gamma=120^\circ$ . The unit cell contains one molecule with submolecules  $j$  at fractional coordinates  $[0,0,(j-1)/s]$ , where  $j=1,\dots,s$ .

Various experimental evidence suggests that molecules often tilt away from the vertical in LB films, in many cases such that the area of the hydrophobic tail projected on to the layer equals the area per hydrophilic head. In the model, tilt is simply imposed. It is specified by giving the angle of tilt  $\theta$  away from the vertical and the plane in which the tilt occurs. All distinct planes of tilt lie between the nearest neighbor (NN) direction ( $AB$  in Fig. 1) and the next-nearest-neighbor (NNN) direction ( $AC$  in Fig. 1). We consider both of these planes of tilt, but molecular dynamics modeling indicates that next-nearest-neighbor tilt is preferred, and we treat this in more detail.

As well as the magnitude and direction of tilt in one layer, the relations between tilts in adjacent layers must be specified. One could imagine complex helical and other structures arising from different sequences of tilts, but the two obvious structures are those in which the tilts are the same in each layer or alternate in sign in successive layers. For the present calculations we have taken the tilts as the same in each layer, so that all layers are identical, as illustrated in Fig. 2.

Deducing the crystal lattice parameters for the tilted structures is an exercise in trigonometry. For nearest-neighbor (NN) tilt, the calculation proceeds with reference to Fig. 3(a). The required angles are

$$\alpha = \angle BOC, \quad \beta = \angle COA, \quad \gamma = \angle AOB, \quad (1)$$

where  $\angle AOB$  is seen to be unchanged by the tilt of the  $c$  axis at  $120^\circ$ . The point  $P$  is the foot of the perpendicular from  $C$  to  $OA$ , extended if necessary. From triangle  $COB$ ,  $\angle COA$  is then seen to be  $90^\circ - \theta$ . The remaining angle is found by repeated application of the cosine rule,

$$\cos \alpha = (OB^2 + OC^2 - BC^2) / 2OB \cdot OC \quad (2)$$

$$= (a^2 + c^2 - BC^2) / 2ac, \quad (3)$$

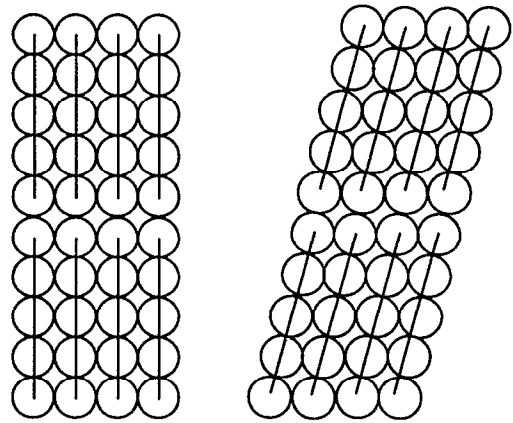


FIG. 2. Untilted and tilted model structures shown in elevation, with equal tilts in successive layers.

$$BC^2 = BP^2 + CP^2 \quad (4)$$

$$= BP^2 + c^2 \cos^2 \theta, \quad (5)$$

$$BP^2 = OB^2 + OP^2 - 2OB \cdot OP \cos 120^\circ \quad (6)$$

$$= a^2 + c^2 \sin^2 \theta - 2ac \sin \theta \cos 120^\circ. \quad (7)$$

Hence substituting back we obtain

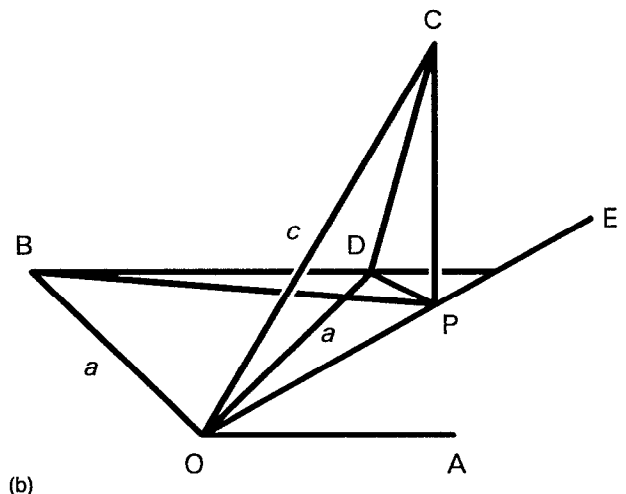
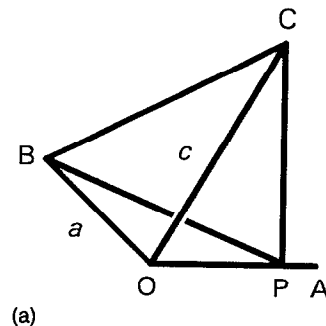


FIG. 3. Unit cell edges and construction for calculating unit cell angles in tilted structures (a) nearest-neighbor (NN) tilt; (b) next-nearest-neighbor (NNN) tilt.

$$BC^2 = a^2 + c^2 + 2ac \sin \theta \cos 120^\circ \quad (8)$$

$$\cos \alpha = \sin \theta \cos 120^\circ \quad (9)$$

$$\alpha = \cos^{-1}(-\frac{1}{2} \sin \theta). \quad (10)$$

This reduces correctly to  $\alpha=90^\circ$  for zero tilt and to  $\alpha=120^\circ$  for  $90^\circ$  tilt, when  $OC$  is parallel to  $OA$  and  $\alpha=\gamma$ .

For next-nearest-neighbor (NNN) tilt, the calculation proceeds with reference to Fig. 3(b). The required angles are again defined as in Eq. (1), and since again only the  $c$  axis tilts,  $\angle AOB$  remains at  $120^\circ$ . The line  $OE$  is the NNN direction and  $P$  is the foot of the perpendicular from  $C$  to  $OE$ , produced if necessary. The line  $OE$  bisects  $\angle AOD$ , which equals  $60^\circ$ , like  $\angle BOD$ , so that  $OE \perp OB$ . Since the plane of tilt is perpendicular to the plane  $AOB$ , it also follows that  $OC \perp OB$  and  $\alpha=90^\circ$ . The remaining  $\angle AOC$  is equal by symmetry to  $\angle DOC$ , which is found by repeated application of the cosine rule,

$$\cos \beta = (OC^2 + OD^2 - CD^2)/2OCOD \quad (11)$$

$$= (c^2 + a^2 - CD^2)/2ca, \quad (12)$$

$$OD^2 = CP^2 + DP^2 \quad (13)$$

$$= c^2 \cos^2 \theta + DP^2, \quad (14)$$

$$DP^2 = OD^2 + OP^2 - 2ODOP \cos 30^\circ \quad (15)$$

$$= a^2 + c^2 \sin^2 \theta - 2ac \sin \theta \cos 30^\circ. \quad (16)$$

Hence substituting back we obtain

$$CD^2 = a^2 + c^2 - 2ac \sin \theta \cos 30^\circ, \quad (17)$$

$$\cos \beta = \sin \theta \cos 30^\circ, \quad (18)$$

$$\beta = \cos^{-1}(\frac{1}{2}\sqrt{3} \sin \theta). \quad (19)$$

This reduces correctly to  $\beta=90^\circ$  for zero tilt and to  $\beta=30^\circ$  for  $90^\circ$  tilt when  $OC \parallel OE$ .

These angles suffice for calculations of the planewise dipole sums from a program that takes input for arbitrary crystal structures. The unit cell edges do not change, remaining  $a$ ,  $a$ , and  $c$  (or  $D$ ,  $D$ , and  $sD$ ), and nor do the submolecule fractional coordinates.

Cartesian tensor components must be referred to a suitable set of orthogonal axes. In our programs the default set is  $a$ ,  $a \times c^*$ , and  $c^*$ . For nearest-neighbor tilt this is adequate; the structure is triclinic and no simplification results from another choice. However, for next-nearest-neighbor tilt the structure is in fact monoclinic, as can be verified by replacing  $a$  by  $OE$ , of length  $\sqrt{3}a$ , giving tilt in the plane  $\perp b$  as is conventional for monoclinic structures. This cell is double the size of the original one and so contains two molecules, with their first submolecules at positions  $(0,0,0)$  and  $(\frac{1}{2}, \frac{1}{2}, 0)$  relative to the monoclinic axes. Use of the monoclinic axes is convenient but not essential; the tensor components relative to the default axes can be transformed to the monoclinic axes in the usual way if required.

This structure is of course idealized. Atomic force microscopy shows that arachidic acid LB films on a silicon

substrate may be distorted from hexagonal packing,<sup>10</sup> while cadmium arachidate LB films on a silicon substrate adopt a rectangular packing.<sup>11</sup> To explore the effect of these differences on planewise dipole sums, we have also performed calculations on model "distorted" structures. One corresponds directly to the monoclinic cell, with the axial ratio  $a/b$  allowed to deviate from the ideal value  $\sqrt{3}$ . The other starts from a square array of side  $D$  corresponding to a tetragonal structure, with the ratio of the axes in the plane allowed to deviate from the ideal value 1.

### III. METHOD

The electric field  $E$  produced at position  $r$  relative to a dipole moment  $p$  is given by

$$E = T \cdot p / 4\pi\epsilon_0, \quad (20)$$

where  $T$  is the dipole tensor  $\nabla\nabla(1/r)$ ; for  $r=0$ ,  $T=0$ . In an electrical or optical field that is uniform over many molecular diameters within a particular layer, all the dipole moments induced are equal. Then the field at a given molecule due to these dipole moments will be determined by the product of the common value of the dipole moments with the sum of the dipole tensor over all the distances between the given molecule and those in the layer. The latter is a planewise or layer dipole sum.

We label successive monolayers  $g(=0,1,\dots)$ , the molecules within a layer  $\lambda$ , and the submolecules within a molecule  $j$  as before. Thus a typical submolecule is located at position  $r(\lambda gj)$ . With this notation, the calculated layer sums are defined as

$$T(gg') = (\nu/4\pi s^2) \sum_{jj'} \sum_{\lambda} T(\lambda gj, 0g'j'), \quad (21)$$

where the summand is the dipole tensor for the vector  $r(\lambda gj) - r(0g'j')$  between two submolecules. The quantity  $\nu$  is the volume per molecule, introduced to make the sums dimensionless, and the factor  $4\pi$  absorbs that in Eq. (20) to simplify later equations. The sum over all pairs of submolecules is divided by the square of the number of submolecules to yield an average molecular interaction; the prime denotes that self-field terms for  $\lambda=0$  and  $g=g'$  are excluded, since a molecule does not polarize itself.

The layer sums are evaluated by the method of de Wette and Schacher<sup>12</sup> with the sign correction noted by Philpott.<sup>4</sup> These expressions treat only point molecules but apply immediately to point submolecules. In particular, different expressions must be used depending on whether or not submolecules  $j$  and  $j'$  lie in the same plane (for which a necessary condition is  $g=g'$ ). The components of the resulting tensors are expressed in an axis system where  $z$  is normal to the layer and tilt occurs in the  $xz$  plane; for NNN tilt, the latter choice conforms with the usual convention for a monoclinic crystal.

Bulk dipole sums are only conditionally convergent; individual terms fall off as the cube of the distance but the number of terms increases as the cube of the distance, leaving the result dependent on the effective shape of the summation volume. However, such sums can be divided into a part dependent only on the shape and a part inde-

TABLE I. Normal components  $L_{zz}$  of the in-layer Lorentz-factor tensor  $L(0)$  as a function of number of submolecules  $s$  for untilted structures.

$s$	1	2	3	4	5	6	7	8	9	10
$L_{zz}$	0.240	0.117	0.065	0.036	0.018	0.006	-0.003	-0.010	-0.015	-0.020

pendent of shape but dependent on the microscopic structure. The shape-independent part, sometimes called a Lorentz-factor tensor<sup>13</sup> or Ewald sum,<sup>4</sup> is of significance in introducing the macroscopic dielectric field into dielectric treatments.<sup>13</sup>

Layer sums correspond to a special choice of summation shape. Nevertheless, the macroscopic field still needs to be introduced into dielectric treatments of layered media. Moreover, the sum of layer sums over layers in a bulk material must yield the bulk sum, corresponding in this case to a slab-shaped summation volume. For this geometry, the bulk Lorentz-factor tensor differs from the bulk dipole sum merely by adding 1 to the  $zz$  component, with  $z$  normal to the slab.<sup>4,13</sup> Hence the layer sums must be such as to conform to this result, and detailed analysis<sup>3</sup> shows that the appropriate layer Lorentz-factor tensors are given by

$$L(gg') = T(gg') + nn\delta_{gg'}, \quad (22)$$

where  $n$  is the unit vector normal to the layers. The present results will be reported as components of  $L$ , which has unit trace since  $T$  has zero trace. For the structures treated here, in which all layers are identical,  $T(gg')$  and  $L(gg')$  depend only on the separation between the layers  $g$  and  $g'$  and not on their absolute position; in other words, they depend only on the difference  $g-g'$  and not on  $g$  and  $g'$  separately.

## IV. RESULTS

### A. Untilted structures

For untilted structures, the main questions concern the effects of the number of submolecules  $s$  and of the separation between layers  $g-g'$ . Although these are not independent, one expects any realistic model to have a value of  $s$  larger than 1 or 2 and for the layer sums then to decrease rapidly with  $g-g'$ . Hence we consider first the dependence on  $s$  for the in-layer sum where  $g=g'$ , i.e., for  $L(0)$ . Symmetry makes  $L_{xx}=L_{yy}$ , and since  $\text{Tr} L=1$  by Eq. (22), it suffices to quote only  $L_{zz}$  to characterize  $L$ , since  $L_{xx}=(1-L_{zz})/2=L_{yy}$ .

The results are shown in Table I. As already remarked,

the structure does not reduce to close packing for  $s=1$  and so the value of  $L_{zz}$  differs from the isotropic value of  $1/3$ . As  $s$  increases,  $L_{zz}$  rapidly decreases to zero and then slowly falls below zero. Similar behavior was observed in previous work.<sup>8</sup> For molecules that are significantly extended, say  $s \geq 5$ , the components of  $L(0)$  are approximately  $(\frac{1}{2}, \frac{1}{2}, 0)$ . These are the depolarization factors for a needle-shaped cavity in a dielectric continuum, which would be the appropriate Lorentz cavity for parallel elongated molecules like those considered here. Since within one layer the dependence on  $s$  is very weak for  $s \geq 5$ , we have chosen  $s=5$  as a value to represent a suitably elongated molecule without excessive computational effort, and  $s=10$  to provide a check.

The calculated values of  $L_{zz}(g)$  for  $s=5$  and  $s=10$  are shown in Table II as a function of  $g$ . From the in-layer sums with  $g=0$  to the adjacent-layer sums with  $g=1$ ,  $L_{zz}$  decreases by about an order of magnitude (and the decrease in  $T_{zz}$  is more than two orders of magnitude). Once  $g=2$ ,  $L_{zz}$  has decreased by many orders of magnitude to become entirely negligible. This behavior is a more extreme version of that found for the anthracene crystal.<sup>14</sup> Within a layer, the dominant contributions come from touching "beads" in neighboring molecules. Between adjacent layers, contributions from touching "beads" in neighboring molecules are equally large but less numerous, while some contributions are much smaller, so that the sum decreases, but not drastically. Beyond adjacent layers, there are no sizable contributions, and the sum is effectively zero.

### B. Tilted structures

Tilted structures for *next-nearest neighbor tilt* have been studied for  $s=5$  and  $s=10$  and for separations between layers  $g=0, 1$ , and  $2$ . For  $g=2$ , the components of the layer Lorentz-factor never exceed  $10^{-10}$ , and so none of these results is quoted. Results for tilts of  $20^\circ$  and  $40^\circ$  are

TABLE III. Components  $L_{\alpha\beta}(g)$  of the layer Lorentz-factor tensor for  $s=5$  submolecules and  $g=0$  and  $1$  as a function of the molecular tilt  $\theta$  from the vertical in the next-nearest-neighbor direction.

$\theta$	$\alpha\beta$			
	$xx$	$xz$	$yy$	$zz$
	$g=0$			
$0^\circ$	0.491	0	0.491	0.018
$20^\circ$	0.440	0.093	0.467	0.093
$40^\circ$	0.281	0.148	0.420	0.299
	$g=1$			
$0^\circ$	-0.0016	0	-0.0016	0.0031
$20^\circ$	0.0010	-0.0023	-0.0007	-0.0002
$40^\circ$	0.0016	0.0011	0.0043	-0.0059

TABLE II. Normal component  $L(g)$  of the layer Lorentz-factor tensor as a function of the separation between layers  $g$  for  $s=5$  and  $10$  submolecules in untilted structures.

$g$	$s=5$	$s=10$
0	0.018	-0.020
1	0.0031	0.0016
2	$< 10^{-12}$	$< 10^{-20}$

TABLE IV. Same as Table III, but for  $s=10$  submolecules.

$\theta$	$\alpha\beta$			
	$xx$	$xz$	$yy$	$zz$
	$g=0$			
$0^\circ$	0.510	0	0.510	-0.020
$20^\circ$	0.454	0.109	0.486	0.061
$40^\circ$	0.279	0.172	0.440	0.281
	$g=1$			
$0^\circ$	-0.0008	0	-0.0008	0.0016
$20^\circ$	0.0005	-0.0012	-0.0004	-0.0001
$40^\circ$	0.0008	0.0005	0.0021	-0.0029

shown in Tables III and IV with those for zero tilt for comparison. The independent nonzero components of  $L$  for the tilted structure are  $L_{xx}$ ,  $L_{xz}=L_{zx}$ ,  $L_{yy}$  and  $L_{zz}$ .

For both  $s=5$  and  $s=10$ , the calculations show how  $L_{xx}(0)$  decreases progressively with tilt while  $L_{zz}(0)$  and  $L_{zz}(0)$  increase. Since tilt takes place in the  $xz$  plane, it has less effect of  $L_{yy}(0)$ , which shows a smaller decrease than  $L_{xx}(0)$ . Between adjacent layers, tilt makes  $L_{xx}(1)$  and  $L_{yy}(1)$  increase steadily, and  $L_{zz}(1)$  decreases and then increases. The components for  $g=1$  are at most 1% of the corresponding component for  $g=0$ , except for  $L_{zz}$  for zero tilt where the result is obscured in adding 1 to  $T_{zz}$ ; in fact,  $T_{zz}(1)$  is also less than 1% of  $T_{zz}(0)$ , as already noted. There are no major differences between  $s=5$  and  $s=10$ , except that for  $g=1$  all the components for  $s=10$  are roughly half those for  $s=5$ .

Tilted structures have also been studied for *nearest-neighbor tilt*. Table V gives results for  $s=5$  and  $g=0$  and 1 as a function of tilt. For  $g=2$ , no component exceeds  $10^{-14}$  and so no results are given. For NN tilt, the symmetry falls to triclinic and  $L(g)$  acquires nonzero  $xy$  and  $yz$  components, but these are too small to be significant. Otherwise, the results are very similar to those in Table III for NNN tilt; note that in each case tilt takes place in the  $xz$  plane, the angle between the planes in the two cases being  $30^\circ$ . Hence the direction of tilt has no major effect on the in-layer sum  $L(0)$  or on the decrease from one layer to the next. Since the results for  $s=5$  are so similar for NN and NNN tilt, while the results for  $s=5$  and  $s=10$  are very similar for NNN tilt, results are not presented for  $s=10$  for NN tilt.

TABLE V. Components  $L_{\alpha\beta}(g)$  of the layer Lorentz-factor tensor for  $s=5$  submolecules and  $g=0$  and 1 as a function of the molecular tilt  $\theta$  from the vertical in the nearest-neighbor direction.

$\theta$	$\alpha\beta$					
	$xx$	$xy$	$xz$	$yy$	$yz$	$zz$
	$g=0$					
$0^\circ$	0.491	0	0	0.491	0	0.018
$20^\circ$	0.442	$-10^{-5}$	0.094	0.464	$10^{-6}$	0.093
$40^\circ$	0.301	$10^{-6}$	0.185	0.363	$-10^{-7}$	0.336
	$g=1$					
$0^\circ$	-0.0016	0	0	-0.0016	0	0.0031
$20^\circ$	0.0012	$10^{-8}$	-0.0022	-0.0011	$-10^{-7}$	-0.0002
$40^\circ$	0.0041	$10^{-7}$	0.0057	-0.0029	$10^{-7}$	-0.0012

### C. Distorted structures

Distortions from the parent hexagonal structure have been explored by calculations for the monoclinic unit cell with the  $a$  dimension increased and the  $b$  dimension decreased by the same proportion, so preserving the unit-cell volume to first order. Distortions of 5% and 10% have been studied for  $s=5$ ,  $g=0$  and 1, and NNN tilts  $\theta=0^\circ$ ,  $20^\circ$ , and  $40^\circ$ . The results are shown in Tables VI and VII.

In the untilted structures, distortion renders the  $x$  and  $y$  directions inequivalent. Since the  $x$  direction is expanded and the  $y$  direction is contracted, the  $xx$  component of  $L$  decreases and the  $yy$  component increases. Making the distortions equal and opposite changes the proportions of the packing in the  $xy$  plane but not, on average, in the  $xz$  and  $yz$  planes. As a result, distortion hardly affects  $L_{zz}$ . In the tilted structures, the interplay of tilt and distortion is complicated. For example, since distortion hardly affects  $L_{zz}$  and  $\text{Tr } L(g)$  is fixed, being 1 for  $g=0$  and zero otherwise, the effect of distortion in reinforcing the change in  $L_{xx}$  due to tilt must simultaneously oppose the corresponding change in  $L_{yy}$  so that  $L_{xx}+L_{yy}$  remains essentially constant. Overall, the distortions used here are seen to have no major effect on the Lorentz-factor tensor; the tilts have a much greater effect.

The effect of changing from the parent hexagonal structure to a parent tetragonal structure with the same cell edges has been explored for  $s=5$ . Results for  $g=0$  and 1 are shown as a function of NN tilt in Table VIII. The less close-packed structure in the  $xy$ -plane compared with the parent hexagonal structure makes  $L_{zz}(0)$  somewhat larger,  $L_{yy}(0)$  somewhat smaller, and the magnitude of  $L(1)$  larger (cf. Table V), but the differences are mainly of detail.

Distortions of 5% and 10% from the parent tetragonal structure have also been investigated. As before, equal and opposite distortions were applied in the  $x$  and  $y$  directions. The results for  $s=5$ , restricted to  $g=0$ , are shown in Table IX. Compared with the parent hexagonal structure, distortion has a more marked effect, and a more complicated one because  $L_{zz}(0)$  is no longer essentially constant. Nevertheless, it remains true that the tilts have the greater effect.

TABLE VI. Components  $L_{\alpha\beta}(g)$  of the layer Lorentz-factor tensor for a 5% distortion for  $s=5$  submolecules and  $g=0$  and 1 as a function of NNN tilt  $\theta$ .

$\theta$	$\alpha\beta$			
	$xx$	$xz$	$yy$	$zz$
	$g=0$			
0°	0.454	0	0.528	0.017
20°	0.411	0.092	0.501	0.089
40°	0.261	0.157	0.440	0.298
	$g=1$			
0°	-0.0018	0	-0.0014	0.0031
20°	0.0012	-0.0024	-0.0007	-0.0005
40°	0.0023	0.0023	0.0034	-0.0057

## V. DISCUSSION

The results presented here provide detailed information on the dipolar interactions in some model Langmuir-Blodgett films. From this information the following conclusions can be drawn. Planewise sums do not depend greatly on the axial ratio of the molecules once this exceeds about 5:1, and hence the present results should be of broad applicability among elongated film-forming molecules. In-layer sums then dominate; interactions with adjacent layers are typically 1% of the corresponding in-layer ones, and interactions with all other layers are negligible. Hence for calculating optical and electrical properties of LB films it should usually suffice to consider only the in-layer sums, with the result that the calculations are greatly simplified; and it should always suffice to consider the in-layer and adjacent-layer sums, which is also an entirely tractable task.

Tilt of the molecules has an important effect on the components of the interaction. It lowers the symmetry, thereby inducing additional nonzero components, and it modifies the original components. The plane of tilt does not greatly affect the interactions. Changing from a hexagonal to a tetragonal parent structure has only minor effects. Distorting from either structure produces rather complicated effects, especially in combination with the effects of tilt, though for the sizes of distortion and tilt studied here, tilt seems the more important factor.

TABLE VII. Components  $L_{\alpha\beta}(g)$  of the layer Lorentz-factor tensor for a 10% distortion for  $s=5$  submolecules and  $g=0$  and 1 as a function of NNN tilt  $\theta$ .

$\theta$	$\alpha\beta$			
	$xx$	$xz$	$yy$	$zz$
	$g=0$			
0°	0.409	0	0.581	0.010
20°	0.371	0.089	0.549	0.080
40°	0.237	0.165	0.473	0.290
	$g=1$			
0°	-0.0021	0	-0.0011	0.0032
20°	0.0015	-0.0027	-0.0007	-0.0008
40°	0.0034	0.0032	0.0026	-0.0060

TABLE VIII. Components  $L_{\alpha\beta}(g)$  of the layer Lorentz-factor tensor for the tetragonal parent structure with  $s=5$  submolecules for  $g=0$  and 1 as a function of the molecular tilt  $\theta$  from the vertical in the nearest-neighbor direction.

$\theta$	$\alpha\beta$			
	$xx$	$xz$	$yy$	$zz$
	$g=0$			
0°	0.481	0	0.481	0.039
20°	0.447	0.104	0.440	0.113
40°	0.296	0.221	0.328	0.376
	$g=1$			
0°	-0.0026	0	-0.0026	0.0052
20°	-0.0030	-0.0031	0.0020	0.0010
40°	0.0059	0.0075	-0.0071	0.0012

As already implied, the planewise dipole sums calculated here are a means to an end and not an end in themselves. They constitute a key ingredient in theories of the optical and electrical properties of LB films, and accordingly they are used in the accompanying paper<sup>5</sup> to calculate linear and nonlinear optical properties of model film structures.

The dipole sums determine the local electric field that polarizes the molecules, so giving rise to the net optical response. This has been considered previously<sup>15</sup> using a crystal model. The quantity corresponding to the planewise sums was derived from calculations<sup>16</sup> for a simple cubic lattice using a quantity  $\xi_0$  equal to  $-9.0336\dots$ . This quantity corresponds to  $4\pi T_{zz}(0)$  in the present notation, and so is equivalent to  $L_{zz}(0)=0.2811\dots$ . This is exactly the value obtained by the present calculations for the tetragonal lattice with  $s=1$ . However, as Table I shows (for the slightly different case of the hexagonal lattice), the value of  $L_{zz}(0)$  for  $s=1$  is not representative of the values for  $s \geq 5$  appropriate to elongated film-forming molecules.

A similar criticism applies to the use of the *isotropic* Lorentz approach, which corresponds to  $L_{xx}=L_{yy}=L_{zz}=1/3$ . The proper approximation in the spirit of the Lorentz approach is to assume a needle-shaped cavity, where as discussed above  $L_{xx}=L_{yy}=1/2$  and  $L_{zz}=0$ . However, this is a reasonable approximation only for vertical molecules in undistorted axial structures, as the tables here

TABLE IX. Components  $L_{\alpha\beta}(g)$  of the in-layer Lorentz-factor tensor for the tetragonal parent structure with  $s=5$  submolecules for 5% and 10% distortions as a function of the molecular tilt  $\theta$  from the vertical in the nearest-neighbor direction.

$\theta$	$\alpha\beta$			
	$xx$	$xz$	$yy$	$zz$
	5% distortion			
0°	0.407	0	0.557	0.036
20°	0.377	0.096	0.521	0.103
40°	0.262	0.216	0.398	0.341
	10% distortion			
0°	0.333	0	0.641	0.026
20°	0.313	0.087	0.600	0.087
40°	0.228	0.207	0.471	0.302

show. The submolecule treatment enables us to take full account of the molecular size, shape and orientation, and to reveal the implications of approximate treatments. It is therefore important in developing realistic theories of film properties.

### ACKNOWLEDGMENTS

This work was supported by DARPA Contract No. DAJA 45-89-C-0036. Some calculations on distorted structures were performed by J. C. Boxall and S. J. Collins.

<sup>1</sup>R. W. Munn, in *Molecular Electronics: Materials and Methods*, edited by P. I. Lazarev (Kluwer, Dordrecht, 1991), p. 1.

<sup>2</sup>R. W. Munn, *Mol. Phys.* **64**, 1 (1988).

<sup>3</sup>R. W. Munn, S. E. Mothersdale, and M. M. Shabat, in *Organic Materials for Nonlinear Optics II*, RSC Special Publication 91, edited by R. A. Hann and D. Bloor (Royal Society of Chemistry, Cambridge, 1991), p. 31.

<sup>4</sup>M. R. Philpott, *J. Chem. Phys.* **58**, 588 (1973); *Adv. Chem. Phys.* **23**, 227 (1973).

<sup>5</sup>R. W. Munn and M. M. Shabat, *J. Chem. Phys.* **99**, 10059 (1993).

<sup>6</sup>M. Bishop, J. H. R. Clarke, L. E. Davis, T. A. King, F. R. Mayers, A. Mohebati, R. W. Munn, M. M. Shabat, D. West, and J. O. Williams, *Thin Solid Films* **210/211**, 185 (1992).

<sup>7</sup>R. W. Munn and M. M. Shabat, in *Molecular Electronics-Science and Technology II*, edited by A. Aviram (American Institute of Physics, New York, 1992), p. 245.

<sup>8</sup>D. A. Dunmur and R. W. Munn, *Chem. Phys.* **76**, 249 (1983).

<sup>9</sup>M. Hurst and R. W. Munn, *J. Mol. Electron.* **2**, 101 (1986).

<sup>10</sup>L. Bourdieu, P. Silberzan, and D. Chatenay, *Phys. Rev. Lett.* **67**, 2029 (1991).

<sup>11</sup>E. Meyer, L. Howald, R. M. Overney, H. Heinzelman, J. Frommer, H.-J. Güntherodt, T. Wagner, H. Schier, and S. Roth, *Nature* **349**, 398 (1991).

<sup>12</sup>F. W. de Wette and G. E. Schacher, *Phys. Rev.* **137**, A78 (1965).

<sup>13</sup>P. G. Cummins, D. A. Dunmur, R. W. Munn, and R. J. Newham, *Acta Crystallogr. A* **32**, 847 (1976).

<sup>14</sup>S. E. Mothersdale and R. W. Munn, *J. Chem. Phys.* **97**, 4536 (1992).

<sup>15</sup>G. Cnossen, K. E. Drabe, and D. A. Wiersma, *J. Chem. Phys.* **97**, 4512 (1992).

<sup>16</sup>A. Bagchi, R. G. Barrera, and R. Fuchs, *Phys. Rev. B* **25**, 7086 (1982).